European Journal of Chemistry 17 (2) (2026) 109-117

European Journal of Chemistry

ATLANTA PUBLISHING HOUSE

Check for updates

View Journal Online
View Article Online

Corrosion inhibition performance of imibenconazole for mild steel in sulfuric acid: A comprehensive investigation

Nayana Kudluru Onkarappa [1], Jeevan Chakravarthy Arakalagudu Satyanarayana [2,*] and Prashanth Shivappa Adarakatti [3]

[1] *Department of Chemistry & Research Centre, Faculty of Nagarathnamma Meda Kasturiranga Rashtriya Vidyalaya College, Bangalore University, Bengaluru-560041, India*
[2] *Department of Chemistry, Faculty of Bhusanayana Mukundadas Sreenivasaiah Institute of Technology & Management, Visvesvaraya Technological University, Bengaluru-560113, India*
[3] *Department of Chemistry, Faculty of Shri Vijay Mahantesh Arts, Science and Commerce College, Ilkal- 587125, India*

* *Corresponding author at: Department of Chemistry, Faculty of Bhusanayana Mukundadas Sreenivasaiah Institute of Technology & Management, Visvesvaraya Technological University, Bengaluru-560113, India.*
e-mail: jeechakravarthy@gmail.com (J.C.A. Satyanarayana).

RESEARCH ARTICLE

10.5155/eurjchem.17.2.109-117.2731

Received: 1 December 2025
Received in revised form: 3 March 2026
Accepted: 10 April 2026
Published online: 30 June 2026
Printed: 30 June 2026

KEYWORDS

Mild steel
Adsorption
Sulfuric acid
Imibenconazole
Corrosion inhibition
Electrochemical analysis

ABSTRACT

In this work, the efficacy of imibenconazole (IB) as a new mild steel corrosion inhibitor in 1 N sulfuric acid is examined. With 95.4-96.6% inhibition at an ideal dose of 500 μM, weight loss measurements show strong inhibitory efficiency. The formation of a protective coating by imibenconazole on the steel surface is demonstrated by scanning electron microscopy (SEM) photographs. Improvements in charge transfer resistance (R_{ct}), a shift in Tafel lines to higher potentials, and a drop-in double-layer capacitance (C_{dl}) are indicative of improved corrosion resistance as measured by electrochemical methods. The inhibitor's adsorption aligns with the Langmuir isotherm, and the values of $\Delta G°_{ads}$ (25-30 kJ/mol) indicate a combined physisorption and chemisorption mode of adsorption. Reliable long-term corrosion prevention is ensured by its durable protective action up to 120 h. Due to its adaptability, the inhibitor can be applied by coatings, injections, and immersions, making it suitable for a range of situations. While stressing the need for more research to examine the applicability of imibenconazole in various materials and situations, the study offers a strong foundation for the adoption of imibenconazole as an efficient corrosion inhibitor. To guarantee long-term protection and effectiveness, routine maintenance and observation are recommended.

Cite this: *Eur. J. Chem.* **2026**, *17(2)*, 109-117 **Journal website**: www.eurjchem.com

1. Introduction

Mild steel (MS) is widely utilized in many industrial sectors due to its many physical qualities and low cost, however, one of the major issues industries face is MS corrosion [1]. Corrosion leads to a number of problems, including environmental problems, costly reestablishment, equipment replacement, and loss of life [2]. The pouring of a 15% HCl solution down steel tubes is a common industrial procedure used to remove scales and accumulated salts from flow channels, such as acidification of oil wells, which increases the production of crude petroleum oil. However, the steel is severely damaged by the aggressive character of the 15% HCl solution, which also deteriorates the steel qualities and restricts its use. Due to these problems, experts focused on the corrosion issue and devised strategies to extend the lifespan of metallic gadgets, machinery, infra-structure, and other items. By using several corrosion protection techniques, such as upgrading materials, applying inhibitors, alloying, using different types of coating, and altering the atmosphere, the degradation of different metals can be greatly reduced. The easiest and most economical way to prevent corrosion among these techniques is to use corrosion inhibitors. By adhering to the metal surface, corrosion inhibitors prevent materials from corroding and exhibit exceptional anticorrosive properties [3]. Oxides, sulfur, nitrogen, and π-bonded compounds are known to be effective corrosion inhibitors in acidic environments [4]. The surface area for interaction with the corrosive media is reduced when the inhibitors are adsorbed on the metal by π and nonbonded electrons in the moiety [5]. As a result, the active sites of the surface are hampered, suppressing corrosion. To stop corrosion in acidic media, corrosion inhibitors are widely employed in a variety of industries.

Corrosion inhibitors are used primarily in the following industries: chemical, heavy industrial manufacturing, water treatment, oil and gas exploration and production, petroleum refining, and additive product manufacture.

ISSN 2153-2249 (Print) / ISSN 2153-2257 (Online)
https://dx.doi.org/10.5155/eurjchem.17.2.109-117.2731

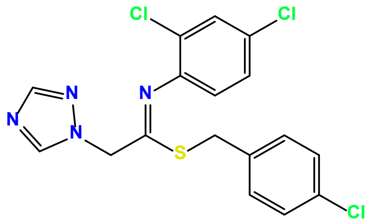

Scheme 1. Structure of (4-chlorophenyl)methyl *N*-(2,4-dichlorophenyl)-2-(1,2,4-triazol-1-yl)ethanimidothioate, (imibenconazole).

Many organic chemicals have been identified as corrosion inhibitors to this day [6], yet the majority are poisonous by nature and work only at higher concentrations [7,8]. The growing awareness of environmental contamination and human health has led scientists to look for anticorrosive substances that are safe, nontoxic, environmentally benign, and have exceptional inhibitory efficiency [9].

The present paper reports the study of the influence of the imibenconazole compound (Scheme 1) on mild steel corrosion in 1 N sulfuric acid. Furthermore, the work has focused on investigating the inhibition mechanism by using potentiodynamic polarization, electrochemical impedance spectroscopy (EIS), and weight-loss corrosion methods. The surface morphologies of the mild steel surface after corrosion have been characterized by scanning electron microscopy (SEM) images. In addition, to know the inhibition action of imibenconazole (IB) corrosion studies were carried out in different corrosion mediums and at different intervals of time by the weight loss method.

2. Experimental

Before inhibition studies, the MS surface was cleaned by soaking in diluted HCl (1 M) for 10 min followed by dipping in NaOH (1 M) solution. The surface was mechanically polished using different grades of emery paper and degreased with trichloroethylene vapors, followed by washing with diluted HCl (1 M) and water. The corrosion medium of different acid such as 1 N H_2SO_4, HCl, HNO_3 and H_3PO_4 solutions were prepared by using distilled water. The temperature was maintained using a thermostat.

The corrosion inhibitor imibenconazole was purchased from Sigma-Aldrich. The stock solution of the inhibitor was prepared by dissolved 180 mg of imibenconazole in 10 mL of 1:1 alcohol and acetic acid mixture in 50 mL standers flask. Using the stock solution 25, 50, 75, 100, 250 and 500 µM concentrations of imibenconazole in 1 N H_2SO_4 acid medium were prepared. Corrosion studies were carried out using a weight loss method and electrochemical methods such as potentiodynamic polarization [10] and AC impedance [11] methods.

The weight loss method is simplest and most widely used method for evaluating the corrosion rates of the materials. Mild steel specimens of area 3×4 cm² were used. Weight loss measurements were carried out at different temperature 301±2, 311±2, 321±2 and 331±2 K in the presence of different inhibitor concentrations 25, 50, 75, 100, 250 and 500 µM. The MS samples were immersed in corrosion medium and the samples were weighed periodically after 3 hours. The samples were removed, washed in running water for about 15 minutes, dried, placed in desiccators to reach room temperature and weighed. The experiments were carried out in triplicate.

The loss in weight so obtained was used to determine the corrosion rate (C_R) by Equation 1 [12].

$$\text{Corrosion rate } (C_R) = \frac{22300\times W}{A\times t\times D} \tag{1}$$

where C_R is the corrosion rate (mpy), A is the initial exposed surface area (cm²), W is the mass loss (mg), t is the exposure time (h) and D is the density of the metal (g/cm³).

Inhibition efficiency (IE %) and surface coverage (θ) were calculated from Equations 2 and 3, respectively [13].

$$\text{Inhibition efficiency } (IE\ \%) = \frac{W_o - W}{W_o} \times 100 \tag{2}$$

where W_0 and W are the weight loss of mild steel without and with the inhibitor in mg, respectively.

$$\text{Surface coverage } (\theta) = \frac{1}{IE\%} \tag{3}$$

The corrosion studies were carried out using an electrochemical method, such as potentiodynamic polarization [10]] and AC impedance [13] methods using an electrochemical analyzer (CH Instrument, H1660C, USA made). The mild steel surface with an exposed surface area of 1×1 cm² serves as working, Pt wire as a counter electrode and saturated calomel electrode (SCE) as a reference electrode, respectively, in conventional three-electrode cell.

The potentiodynamic polarization studies were carried out at open circuit potential (OCP) at a rate of 10 mV/s and in the current range of -20 to 20 mV from OCP. The corrosion current (I_{corr}) is determined by extrapolating the cathodic and anodic Tafel lines [14].

Electrochemical impedance spectra were recorded at the OCP in the frequency range of 100 kHz to 10 mHz with an AC amplitude of 5 mV. The same cell and system were used as in the polarization method [13]. Various impedance parameters are determined, such as charge transfer resistance (R_{ct}), solution resistance (R_S), double layer capacitance (C_{dl}) [15]. Niquist plots for the study are given [16].

The surface morphology of the MS specimen after weight loss measurement in the presence and absence of inhibitor has been analyzed using scanning electron microscope images (Zeiss Sigma 300 FESEM, Germany).

3. Results and discussion

3.1. Inhibition studies in different acid medium

Weight loss measurements are performed in 1 N H_2SO_4, HNO_3, HCl, and H_3PO_4 medium in the presence and absence of IB to determine the influence of inhibitor on the corrosion rate in various acid media (Table 1) [17]. IB increases corrosion in HNO_3, as evidenced by the increased corrosion rate seen in 1 N nitric acid compared to blank. On the other hand, IB inhibits mild steel corrosion in the presence of sulfuric, hydrochloric, and orthophosphoric acid by demonstrating lower CR values for the inhibitor solution compared to the blank. 1 N H_2SO_4 showed the strongest inhibition about 89.6%, whereas H_3PO_4 showed the maximum inhibition about 95%. Since sulfuric acid is a potent acid with many uses, more research is being done in 1 N H_2SO_4. The inhibition mechanism was investigated along with optimization of inhibitor concentration and time.

Table 1. Corrosion rate and percentage inhibition in the different acids in presence and absence of a 500 µM imibenconazole inhibitor.

Acids	**$C_R\times10^2$ (mpy)**		***IE* (%)**
	Blank	**Imibenconazole**	
H_2SO_4	19.89	1.74	+89.60
HNO_3	60.30	100.25	-66.07
HCl	0.58	0.194	+66.60
H_3PO_4	2.32	0.097	+95.00

Table 2. Corrosion parameters from weight loss measurement at different temperature and concentration of imibenconazole.

Inhibitorconcentration(µM)	**301 K**			**311 K**			**321 K**			**331 K**		
	$C_R\times10^3$ (mpy)	***IE* (%)**	**θ**	**$C_R\times10^3$ (mpy)**	***IE* (%)**	**θ**	**$C_R\times10^3$ (mpy)**	***IE* (%)**	**θ**	**$C_R\times10^3$ (mpy)**	***IE* (%)**	**θ**
Blank	2.028	-	-	3.100	-	-	3.569	-	-	8.730	-	-
25	1.242	38.70	0.0258	2.308	31.12	0.0321	2.063	24.16	0.0413	7.104	18.66	0.0535
50	0.873	56.93	0.0175	1.550	50.66	0.0197	1.890	45.83	0.0218	4.890	44.00	0.0227
75	0.388	80.83	0.0123	0.757	75.62	0.0132	1.125	67.77	0.0147	3.901	55.33	0.0180
100	0.203	89.05	0.0111	0.436	85.93	0.0116	0.698	80.00	0.0125	2.542	70.88	0.0141
250	0.106	94.73	0.0105	0.232	92.50	0.0108	0.446	87.22	0.0114	2.018	76.88	0.0130
500	0.067	96.58	0.0103	0.145	95.32	0.0104	0.242	93.05	0.0125	0.766	91.22	0.0109

3.2. Effect of inhibitor concentration and temperature on mild steel corrosion

At 301±2, 311±2, 321±2, and 331±2 K, the weight loss method was used with varying inhibitor doses of 25, 50, 75, 100, 250, and 500 µM. After being suspended for three hours, the mild steel specimens in 1 N H_2SO_4. The difference between the weights of the samples prior to and after immersion was used to calculate weight loss. The trials were carried out three times and the average of the three findings was calculated. Using the formulae, the inhibition efficiency (*IE*%) and surface coverage (θ) were determined [14].

By measuring weight loss at 301 K after a 3 hour immersion, the impact of adding imibenconazole (IB) at different doses on mild steel corrosion was investigated in a solution of 1 N H_2SO_4. Table 2 lists the inhibition efficiency (*IE*%) and corrosion rates (C_R) for imibenconazole at various doses in 1 N H_2SO_4 derived from weight loss measurements. It has been discovered that while the corrosion rate reduces with increasing inhibitor concentration, the inhibition efficiency increases [18]. The adsorption of the inhibitors at the mild steel/acid solution interface is responsible for the suppression of mild steel corrosion. At 500 µM concentration, imibenconazole exhibits more than 96.58% inhibition efficiency, making it a good inhibitor. Imibenconazole's potent anti-corrosion properties for mild steel in 1 N H_2SO_4 solutions could be attributed to the heteroatoms and aromatic rings present in its structures [19]. The good corrosion inhibition at micromolar concentration of inhibitor molecule is more beneficial which convey a little ecological harm due to IB.

By measuring weight loss at various temperatures (301, 311, 321, and 331 K) with and without imibenconazole (IB) at varying concentrations, the impact of temperature on the effectiveness of IB as corrosion inhibitors is examined. The values of corrosion rate (C_R) and inhibition efficiency (*IE*%) derived from weight loss experiments at various temperatures are displayed in Table 2. According to Table 2 data, IB adsorbed on the mild steel surface occurs at all investigated temperatures, and corrosion rates in both inhibited and uninhibited solutions rise with temperature.

An increase in temperature typically speeds up corrosion reactions that lead to a faster metal dissolution rate under acidic conditions [20]. Metal corrosion is usually accompanied by the development of H_2 gas [21]. Table 2 shows that the inhibitory efficacy reduces marginally when the temperature increases from 301 to 331 K. The adsorbed inhibitor coating of the mild steel surface may be deteriorating, which could explain a small drop in inhibitor efficacy with temperature. These findings demonstrate that within the temperature range under investigation, IB is a highly effective inhibitor of mild steel corrosion in 1 N H_2SO_4. The strong interaction between the mild steel surface and inhibitor molecules is responsible for the outstanding results of the tested IB [13].

3.3. Adsorption isotherm and thermodynamic parameters

First, organic inhibitor molecules must adsorb at the metal/solution interface. The adsorption process depends on the temperature, the electrochemical potential at the interface, and the chemical makeup of the molecules. This inhibits metallic corrosion [22,23]. Adsorption of solvent molecules by metal/solution contact is actually possible. For this reason, it is possible to think of the adsorption of organic inhibitor molecules from the aqueous solution as a quasi-substitution process between the water molecules at the electrode surface [$H_2O_{(ads)}$] and the organic compounds in the aqueous phase [$Org_{(sol)}$] (Equation 4) [24].

$$\mathrm{Org}_{(\mathrm{sol})} + \mathrm{xH_2O}_{(\mathrm{ads})} \leftrightarrow \mathrm{Org}_{(\mathrm{ads})} + \mathrm{xH_2O}_{(\mathrm{sol})} \tag{4}$$

where x is the size ratio, that is, the number of water molecules replaced by an organic inhibitor. The adsorption isotherm may offer fundamental details about the inhibitor's interaction with the mild steel surface. To derive the isotherm, one must determine the linear relationship between inhibitor concentration (C_{inh}) and degree of surface coverage (θ) (Table 2). Fitting the h values to isotherms, such as Langmuir [25], Temkin [26], Frumkin [27], and Flory-Huggins [28] isotherms, was attempted. By far the best fit is obtained with the Langmuir isotherm. According to this isotherm, θ is related to C_{inh} by Equation 5.

$$\frac{C_{inh}}{\theta} = \frac{1}{K_{ads}} + C_{inh} \tag{5}$$

where K_{ads} denotes the equilibrium constant for the adsorption process of inhibitor.

In Figure 1, the plots of C_{inh}/θ *vs* C_{inh} are shown and for every concentration and at every temperature, the predicted linear connection is found. Strong correlations (R^2 = 0.998 for 301 K, R^2 = 0.997 for 311 K, R^2 = 0.998 for 321 K, and R^2 = 0.998 for 331 K) support the applicability of this methodology. The slopes of the straight lines suggest that there is an interaction between the adsorbed inhibitor molecules and that they form a monolayer on the mild steel surface [25].

Table 3 displays the values of K_{ads} derived from the Langmuir adsorption isotherm as well as the values of the Gibbs free energy of adsorption (ΔG°_{ads}) arrived at using the following Equation 6.

$$\Delta G^\circ{}_{ads} = -R \times T \times \ln(55.5 \times K_{ads}) \tag{6}$$

Table 3. Thermodynamic parameters for the adsorption of imibenconazole at different temperatures.

Temperature (K)	K_{ads} (L/mol)	$\Delta G°_{ads}$ (kJ/mol)
301	559.7	-25.88
311	531.0	-26.61
321	510.0	-27.36
331	531.0	-28.32

Table 4. Thermodynamic activation parameters for corrosion at different imibenconazole concentrations.

Concentration of inhibitor (µM)	E_a (kJ/mol)	λ (mg/cm²)
Blank	42.62	10.67
25	44.80	10.87
50	48.78	11.36
75	56.29	14.19
100	69.69	14.31
250	72.76	14.62
500	75.01	14.69

Table 5. Corrosion rate and percentage inhibition variation with time in the presence and absence of 100 µM IB inhibitor in 1 N H_2SO_4 at room temperature.

Exposure time (h)	$C_R \times 10^3$ (mm/y)		IE (%)
	Blank	Imibenconazole	
1	0.335	0.00297	87.5
2	0.341	0.00294	87.8
3	0.345	0.00287	88.1
4	0.347	0.00279	88.9
5	0.349	0.00282	88.6
6	0.352	0.00285	88.3
7	0.379	0.00298	87.4
24	0.454	0.00305	86.6
48	0.455	0.00309	86.2
72	0.455	0.00314	85.9
96	0.456	0.00318	85.6
120	0.457	0.00330	84.4

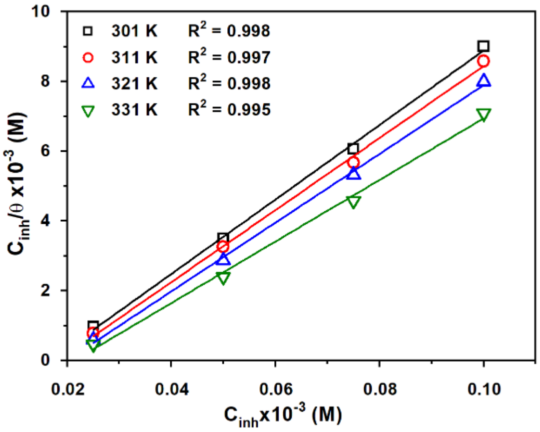

Figure 1. Langmuir adsorption isotherms for IB at different temperatures in 1 N H_2SO_4, obtained from weight loss data.

where R is the universal gas constant, T is the temperature in Kelvin and the value of 55.5 is the concentration of water in the solution mol/L [29].

In 1 N H_2SO_4 solution, the higher adsorption on the mild steel surface is shown by the high K_{ads} values for the investigated imibenconazole. The heteroatoms and π-electrons of the inhibitor molecules provide an explanation for this. A stronger and more stable adsorbed layer forms with higher K_{ads} values (≥100 1/M), increasing inhibition efficiency [30]. These results corroborate imibenconazole's effective anticorrosion properties for mild steel in 1 N H_2SO_4.

The durability of the adsorbed layer on the mild steel surface and the spontaneity of the adsorption process are supported by the negative values of $\Delta G°_{ads}$, which were calculated using Equation 6 [30]. Energy values of 40 kJ/mol or more negative indicate charge sharing or transfer from the inhibitor molecules to the metal surface to form a coordinate covalent bond, or chemisorption [31]. In general, energy values of 20 kJ/mol or less are associated with an electrostatic interaction between charged molecules and the charged metal surface, or physisorption [32]. In this investigation, the $\Delta G°_{ads}$ values found for imibenconazole in mild steel in 1 N H_2SO_4 solution range from 25 to 28 kJ/mol, which is less than 20 kJ/mol (Table 5); this suggests that the adsorption is of mixed complex type, meaning that both physisorption and chemisorption are involved in the adsorption of inhibitor molecules on the surface of mild steel in this study, with chemisorption being the predominant mode of adsorption. The results of the temperature dependence of the inhibitory mechanism (Table 4) support this hypothesis. With increasing temperature, imibenconazole's $\Delta G°_{ads}$ value increases [30-33].

An enhanced interaction between inhibitor molecules and surface iron atoms at elevated temperatures is indicated by the increase in $\Delta G°_{ads}$ values [30]. The percentage inhibition efficiency (Table 2), which only slightly decreases (from 94 to 87%) with increasing temperature, lends more credence to this. Between 96.5 and 95.38, the *IE%* falls. Therefore, we deduce that imibenconazole adsorption in mild steel in 1 N sulfuric acid is mainly chemisorption and complicated in character [34].

The apparent activation energy for the corrosion process is calculated using Arrhenius Equation 7.

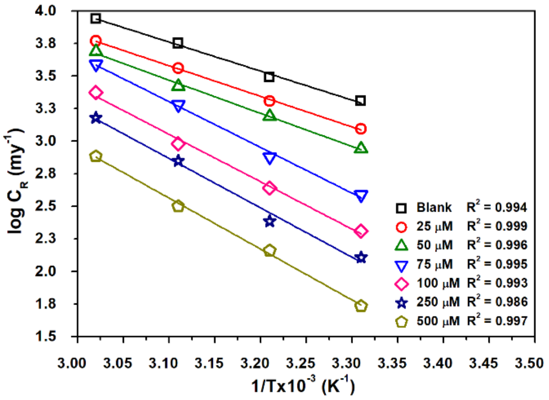

Figure 2. Arrhenius plots related to the variation of the corrosion rate of mild steel with temperature at different concentrations of IB in 1 N H_2SO_4.

$$C_R = \lambda \times \exp(-\frac{E_a}{R \times T}) \quad (7)$$

where E_a is the apparent activation energy for the corrosion process, R is the universal gas constant, T is the absolute temperature and λ is the Arrhenius pre-exponential factor. The corrosion rate is determined by weight loss measurements. Since the value of E_a is in line with the activation of hydrogen ions, it can be considered confirmation that the corrosion process is cathodically controlled [35].

Table 4 presents the apparent activation energies (E_a) and the pre-exponential factor (λ) at a 500 μM concentration of IB as calculated by linear regression between log C_R and $1/T$ (Figure 2). Since all the linear regression coefficients are nearly equal to one, the kinetic model may be able to explain mild steel corrosion in a 1 N H_2SO_4 solution. Table 4 shows that the E_a values of the inhibited solution (43.78-75.09 kJ/mol) are greater than those of the uninhibited solution (42.6 kJ/mol). Equation 7 makes it abundantly evident that a lower corrosion rate is caused by a higher E_a and a lower λ.

The influence of E_a on mild steel corrosion is generally greater than the effect of λ. Because the values of λ and E_a in this study vary in a similar way, the combined influence of λ and E_a causes the corrosion rate to increase with temperature [30].

3.4. Effect of immersion time on corrosion of mild steel

Weight loss measurements were made in 1 N H_2SO_4 with and without inhibitors at 100 μM for varying immersion times of 1 hour at 301 K in order to evaluate the durability of inhibitory behavior on a time scale. Table 5 shows the inhibition efficiencies with immersion time. The inhibition efficiency of IB increases marginally for the first four hours of immersion in inhibited solutions, following which it decreases for the next seven hours. The decrease in inhibition efficiency was observed at 24 and 48 hours of immersion. Due to a decrease in adsorption and an increase in desorption, inhibitory efficacy dropped after 120 hours (5 days). According to Shriver *et al.* [36], the reason for the decrease in inhibition during an extended period of immersion is the chelate formation between iron and the inhibitor ligands, which depletes the available inhibitor molecules in the solution.

3.5. Analysis of the corrosion inhibition mechanism

Mostly through adsorption on the mild steel surface, where it transfers H_20 molecules and forms a tight barrier layer, organic chemical inhibitors stop mild steel corrosion [37]. A chemical bond typical of chemical adsorption is formed when an electron from an inhibitor functional group, such as OH^- or SO_4^{2-}, donates to the d orbital of Fe [38]. In addition, in the presence of imibenconazole, there is a donor- acceptor interaction between the -N=N-, -C=N- and -C=C- π-electrons of IB and the empty orbitals of the iron atom, resulting in a chemisorption phenomenon [39]. Other factors that may influence adsorption include the potential electronic density and the steric effect of active centers, such as aromatic rings, Cl, N, and S. However, when the mild steel sample is submerged in an aqueous acid solution, its surface is positively charged [40]. The mild steel sample is adsorbed with SO_4^{2-} ions, which cause the surface to become negatively charged [41]. Electrostatic attraction causes the protonated inhibitor metal-organic molecules (cationic) to be adsorbed on the negatively charged metal surface. Physical adsorption may arise from protonated molecules adhering to mild steel samples [13]. Imibenconazole is superior to triazole as an inhibitor due to its enhanced adsorption properties, leading to the formation of a more stable and protective layer on metal surfaces. Its molecular structure, which features additional functional groups, offers better interaction and bonding with the substrate in comparison to triazole. Furthermore, imibenconazole exhibits higher chemical stability and corrosion resistance, making it more effective in diverse and harsh environments [42,43].

3.6. Surface morphology studies

Using scanning electron microscopy (SEM), the surface morphology of mild steel was examined. After measuring weight loss in sulfuric acid for three hours, both with and without an inhibitor, Figure 3 displays SEM pictures of the mild steel surface. A photomicrograph of mild steel samples that had corroded in H_2SO_4 without inhibitor IB showed more cracks and pits as a result of the attack of aggressive corrosive medium (Figure 3a) [13]. Because an inhibitor layer has been adsorbed on the mild steel surface, the photomicrograph of the corroded sample in H_2SO_4 containing Inhibitor IB (Figure 3b) revealed fewer corrosion products and a smoother and less cracked metal surface.

3.7. Tafel polarization studies

The temperature of the entire apparatus was kept at 301 K. After the solution was deaerated for roughly 20 minutes, the working electrode was kept at its corrosion potential for 10 minutes, or until a steady state was reached, at which point the polarization curves were recorded. At 301 K, the specimens were subjected to a range of IB concentrations (25 to 500 μM) in 100 mL of 1 M H_2SO_4. Equation 8 was used to calculate the inhibition efficiency ($IE\%$) [44].

Table 6. Potentiodynamic polarisation parameters for corrosion of mild steel in presence of IB in 1 N H_2SO_4

Concentration of imibenconazole (µM)	E_{corr} (V vs. SCE)	β_a (mV/dec)	β_c (mV/dec)	I_{corr} (µA/cm²)	IE (%)
Blank	-0.502	9.32	8.85	26.48	-
25	-0.499	8.26	7.98	18.11	31.00
50	-0.493	6.84	5.56	9.28	64.95
75	-0.484	5.38	5.12	5.79	78.13
100	-0.475	5.11	4.42	4.87	81.60
250	-0.489	4.93	4.09	3.33	87.42
500	-0.447	3.72	2.60	2.39	91.44

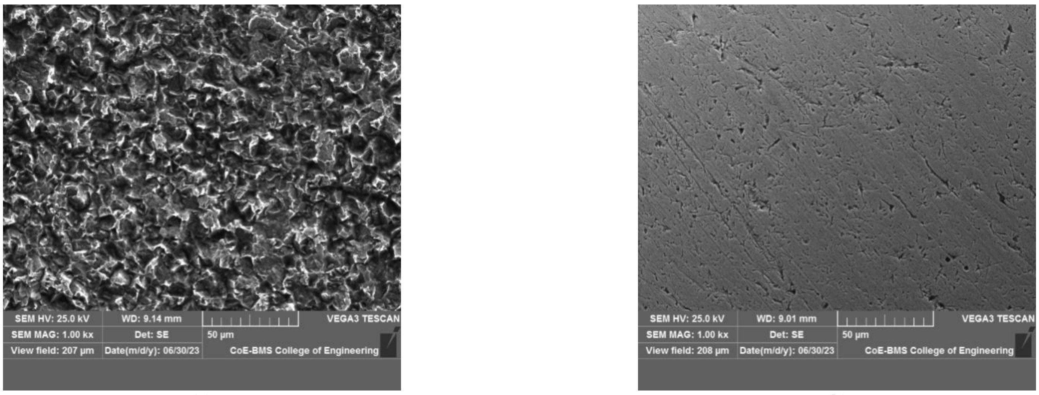

(a) (b)

Figure 3. SEM images of the mild steel surface after 3 h of immersion in 1 N H_2SO_4 in (a) absence and (b) presence of 500 µM of IB.

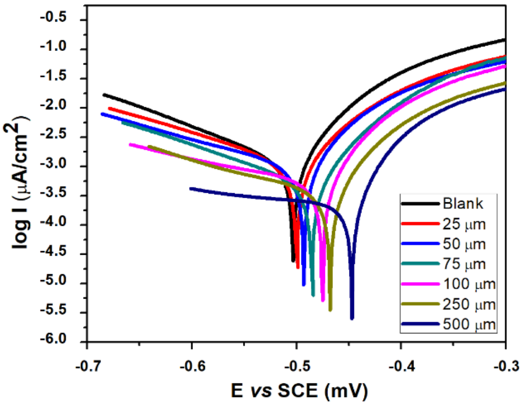

Figure 4. Potentiodynamic polarization plots for corrosion of mild steel in presence of various concentrations of IB in 1 N H_2SO_4.

$$IE\% = \frac{I_o - I}{I_o}\, 100 \qquad (8)$$

where I_o and I are the corrosion current density without and with the inhibitor, respectively.

Potentiodynamic current-potential curves can be obtained by plotting the logarithm of current against the change in electrode potential between -250 and +250 mV from open circuit potential at scan rate. The anodic and cathodic slopes (β_c from open circuit potential β_a), corrosion potential (E_{corr}), and the corrosion current density (I_{corr}) are estimated using established methodologies based on the Tafel curves produced by plotting E vs. log I (Figure 4) [13,46].

Figure 4 shows the mild steel anodic and cathodic polarization curves in acidic conditions with and without inhibitors at varying concentrations. Table 6 includes and calculates the electrochemical parameters E_{corr}, β_c, β_a, and I_{corr}. Because an adsorbed layer forms on the metal surface upon the addition of IB, the corrosion current density I_{corr} falls. Therefore, the inclusion of the inhibitor suppresses the dissolution of metal at the anode and the development of hydrogen at the cathode by affecting both the anodic and cathodic slopes. Thus, the inhibitor has an effect on the kinetics of both cathodic and anodic reactions. IB acts as a mixed type of inhibitor [13]. According to Table 6, the addition of IB causes an increase in the anodic Tafel slopes, suggesting that the hydrogen evolution reaction is activation-regulated. From Equation 8, the percentage inhibition efficiency (IE %) is determined.

At 500 µM of inhibitor, the maximum inhibition efficiency of 91.44% was achieved. The inhibitor functions as a mixed type inhibitor with predominately anodic in 1N H_2SO_4 solution because it inhibits both cathodic hydrogen evolution processes and anodic metal dissolution [47]. According to the polarization investigations, the corrosion potential E_{corr} does not vary as the IB concentration increases, indicating that the inhibitor is a mixed-type inhibitor. Corrosion is suppressed when the concentration of the inhibitor increases because more of the inhibitor is adsorbed onto the metal surface.

3.8. Electrochemical impedance spectroscopy (EIS)

Before each impedance analysis, 1 cm² MS electrode was allowed to attend steady-state open circuit potential for 600 s. Furthermore, at the open-circuit potential and 301 K temperature, impedance measurements were performed. The recorded data have been analyzed using ZSimp-Win 3.21 software.

The EIS data was displayed as the Nyquist plot ($-Z''$ versus Z') (Figure 5a). The electrical circuit proposed to simulate impedance data is shown in Figure 5b and impedance parameters are listed in Table 7.

Table 7. EIS parameters for MS corrosion in presence of IB and 1 N H_2SO_4.

Concentration of imibenconazole (μm)	R_s (Ω.cm²)	R_{ct} (Ω.cm²)	C_{dl} (μF/cm²)	n	IE (%)
Blank	1.30	27.99	34.09	1.00	-
25	1.39	37.21	24.22	1.00	35.7
50	1.90	95.00	12.80	1.00	70.5
75	1.60	162.18	12.00	0.80	82.7
100	1.50	179.00	8.78	0.81	84.3
250	1.45	238.30	6.35	0.85	88.2
500	1.54	297.00	6.03	0.83	90.5

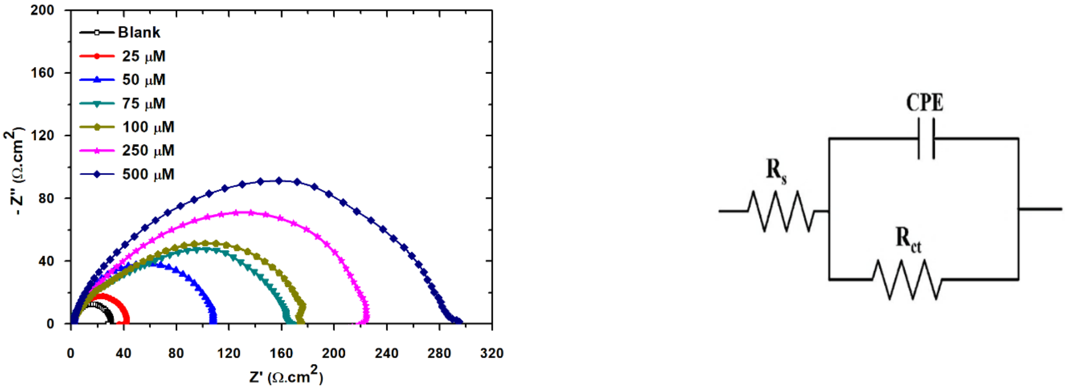

(a) (b)

Figure 5. (a) Nyquist plot for various concentration of IB and (b) Equivalent circuit.

In place of capacitance element, C_{dl} constant phase elements (CPE), have been used because of the distribution of activity centers, the roughness and inhomogeneity of the electrode surface, the adsorption of inhibitors, and the creation of porous layers [48,49]. In the proposed electrical equivalent circuit, R_S is the electrolyte resistance, C_{dl} is the double-layer capacitance, and R_{ct} is the charge transfer resistance. The impedance diagrams (Figure 5a) are perfect semicircles, as shown by the Nyquist plots, suggesting a charge transfer mechanism that primarily regulates steel corrosion. The perfect semicircle is frequently used to describe frequency dispersion [50]. Mild steel is prevented from corroding as the diameter of the semicircle grows proportionally to the IB concentration. Using Equation 9, the percentage inhibition efficiency (*IE%*) was determined.

$$IE(\%) = \frac{R_{ct} - R'_{ct}}{R_{ct}} \times 100 \qquad (9)$$

where R'_{ct} and R_{ct} are the charge transfer resistance of mild steel without and with the inhibitor, respectively.

The inhibitory efficiency from Equation 9 can be computed using the charge transfer resistance, which is a representation of the corrosion resistance. Figure 5b shows the analogous circuit model that was used to simulate the Nyquist plot. As the IB concentration increases, the C_{dl} values fall. This happens because the electrical double layer thickness increases or the local dielectric constant decreases, indicating the creation of an adsorbed layer on the surface of mild steel. A similar trend in inhibition efficiency values is observed in both impedance analysis and Tafel polarization studies, although the values show a slight variation. At 500 μM of the inhibitor, the maximal inhibition efficiency of 90.57% was achieved.

4. Conclusions

The investigation validates the effectiveness of imibenconazole in 1 N H_2SO_4 as a mild steel corrosion inhibitor. Measurement of weight loss indicates that the inhibitor achieves high inhibitory efficacy (95.4-96.6%) at an ideal concentration of 500 μM. Imibenconazole creates protection to the steel surface, as seen in scanning electron microscopy (SEM) images. On the other hand, Tafel lines shift to higher potentials in electrochemical measurements, indicating enhanced corrosion resistance, and there is a decrease in double-layer capacitance (C_{dl}) and an increase in charge transfer resistance (R_{ct}). The inhibitor's adsorption adheres to the Langmuir isotherm, and the thermodynamic variable $\Delta G°_{ads}$ values (ranging from 25 to 30 kJ/mol) indicate a combined physisorption and chemisorption mode of adsorption.

Moreover, a satisfactory inhibition efficiency at the micromolar concentration of IB suggests that the inhibitor poses no ecological harm. IB protection action even after 120 h makes it a good corrosion inhibitor, over a period of more than 5 days. Due to its versatility, imibenconazole can be applied in a variety of ways, including coatings, injections, and immersions, demonstrating its adaptability in a range of situations. All things considered, the study offers a solid basis for the use of imibenconazole as an efficient corrosion inhibitor, but it also emphasizes the need for more investigation to determine the suitability of imibenconazole for use with other materials and in a variety of settings. To guarantee long-term protection and effectiveness, routine maintenance and monitoring are essential.

Acknowledgements

We thank the Government Science College, Nrupathunga University, and the Department of Chemistry, Bangalore University, Bengaluru, India, for providing the laboratory facilities.

Disclosure statement DS

Conflict of interests: The authors declare that they have no conflict of interest.
Ethical approval: All ethical guidelines have been adhered to.
Sample availability: Samples of the compounds are available from the author.

CRediT authorship contribution statement CR

Conceptualization: Nayana Kudluru Onkarappa, Prashanth Shivappa Adarakatt; Methodology: Nayana Kudluru Onkarappa, Jeevan Chakravarthy Arakalagudu, Satyanarayana; Software: Nayana Kudluru Onkarappa, Prashanth Shivappa Adarakatti; Validation: Jeevan Chakravarthy Arakalagudu Satyanarayana, Prashanth Shivappa Adarakatt; Formal Analysis: Nayana Kudluru Onkarappa, Prashanth Shivappa Adarakatt; Investigation: Nayana Kudluru Onkarappa, Prashanth Shivappa Adarakatt; Resources: Nayana Kudluru Onkarappa, Jeevan Chakravarthy Arakalagudu, Satyanarayana; Data Curation: Nayana Kudluru Onkarappa, Jeevan

Chakravarthy Arakalagudu, Satyanarayana; Writing - Original Draft: Nayana Kudluru Onkarappa, Prashanth Shivappa Adarakatt; Writing - Review and Editing: Nayana Kudluru Onkarappa, Prashanth Shivappa Adarakatt; Visualization: Chakravarthy Arakalagudu Satyanarayana, Prashanth Shivappa Adarakatt; Funding acquisition: Chakravarthy Arakalagudu Satyanarayana, Prashanth Shivappa Adarakatt; Supervision: Chakravarthy Arakalagudu Satyanarayana, Prashanth Shivappa Adarakatt; Project Administration: Nayana Kudluru Onkarappa, Jeevan Chakravarthy Arakalagudu, Satyanarayana.

ORCID and Email

Nayana Kudluru Onkarappa
konayana@gmail.com
https://orcid.org/0000-0002-5955-6340
Jeevan Chakravarthy Arakalagudu Satyanarayana
jeechakravarthy@gmail.com
https://orcid.org/0000-0003-0613-2525
Prashanth Shivappa Adarakatti
prashanthsa143@gmail.com
https://orcid.org/0000-0002-9049-4862

References

[1]. Ahamad, I.; Prasad, R.; Quraishi, M. Thermodynamic, electrochemical and quantum chemical investigation of some Schiff bases as corrosion inhibitors for mild steel in hydrochloric acid solutions. *Corros. Sci.* **2010**, *52* (3), 933–942.

[2]. Singh, P.; Ebenso, E. E.; Olasunkanmi, L. O.; Obot, I. B.; Quraishi, M. A. Electrochemical, theoretical, and surface morphological studies of corrosion inhibition effect of green naphthyridine derivatives on mild steel in hydrochloric acid. *J. Phys. Chem. C Nanomater.* Interfaces **2016**, *120*, 3408–3419.

[3]. Yilmaz, N.; Fitoz, A.; Ergun, U.; Emregül, K. C. A combined electrochemical and theoretical study into the effect of 2-((thiazole-2-ylimino)methyl)phenol as a corrosion inhibitor for mild steel in a highly acidic environment. *Corros. Sci.* **2016**, *111*, 110–120.

[4]. Cui, M.; Ren, S.; Xue, Q.; Zhao, H.; Wang, L. Carbon dots as new eco-friendly and effective corrosion inhibitor. *J. Alloys Comp* **2017**, *726*, 680–692.

[5]. Daoud, D.; Douadi, T.; Hamani, H.; Chafaa, S.; Al-Noaimi, M. Corrosion inhibition of mild steel by two new S-heterocyclic compounds in 1 M HCl: Experimental and computational study. *Corros. Sci.* **2015**, *94*, 21–37.

[6]. Singh, A. K.; Thakur, S.; Pani, B.; Ebenso, E. E.; Quraishi, M. A.; Pandey, A. K. 2-Hydroxy-*N*′-((Thiophene-2-yl)methylene)benzohydrazide: Ultrasound-Assisted Synthesis and Corrosion Inhibition Study. *ACS. Omega* **2018**, *3* (4), 4695–4705.

[7]. Chaitra, T. K.; Mohana, K. N.; Tandon, H. C. Thermodynamic, electrochemical and quantum chemical evaluation of some triazole Schiff bases as mild steel corrosion inhibitors in acid media. *J. Mol. Liq.* **2015**, *211*, 1026–1038.

[8]. ElBelghiti, M.; Karzazi, Y.; Dafali, A.; Hammouti, B.; Bentiss, F.; Obot, I.; Bahadur, I.; Ebenso, E. Experimental, quantum chemical and Monte Carlo simulation studies of 3,5-disubstituted-4-amino-1,2,4-triazoles as corrosion inhibitors on mild steel in acidic medium. *J. Mol. Liq.* **2016**, *218*, 281–293.

[9]. El-Etre, A.; Abdallah, M.; El-Tantawy, Z. Corrosion inhibition of some metals using lawsonia extract. *Corros. Sci.* **2005**, *47* (2), 385–395.

[10]. Al-Amiery, A.; Kadhum, A.; Alobaidy, A. H.; Mohamad, A.; Hoon, P. Novel Corrosion Inhibitor for Mild Steel in HCl. *Materials* **2014**, *7* (2), 662–672.

[11]. Bentiss, F.; Lagrenee, M.; Traisnel, M.; Hornez, J. C. The corrosion inhibition of mild steel in acidic media by a new triazole derivative. *Corros. Sci.* **1999**, *41*, 789–803.

[12]. Oparaodu, K. O.; Okpokwasili, G. Comparison of percentage weight loss and corrosion rate trends in different metal coupons from two soil environments. *Int. J. Environ. Bioremediat. Biodegrad.* **2014**, *2*, 243–249. https://pubs.sciepub.com/ijebb/2/5/5/

[13]. Pavithra, M.; Venkatesha, T.; Vathsala, K.; Nayana, K. Synergistic effect of halide ions on improving corrosion inhibition behaviour of benzisothiozole-3-piperizine hydrochloride on mild steel in 0.5M H2SO4 medium. *Corros. Sci.* **2010**, *52* (11), 3811–3819.

[14]. Loto, R. T. Surface coverage and corrosion inhibition effect of Rosmarinus officinalis and zinc oxide on the electrochemical performance of low carbon steel in dilute acid solutions. *Results Phys.* **2018**, *8*, 172–179.

[15]. Ouakki, M.; Galai, M.; Rbaa, M.; Abousalem, A. S.; Lakhrissi, B.; Touhami, M. E.; Cherkaoui, M. Electrochemical, thermodynamic and theoretical studies of some imidazole derivatives compounds as acid corrosion inhibitors for mild steel. *J. Mol. Liq.* **2020**, *319*, 114063.

[16]. Mamudu, U.; Santos, J. H.; Umoren, S. A.; Alnarabiji, M. S.; Lim, R. C. Investigations of corrosion inhibition of ethanolic extract of Dillenia suffruticosa leaves as a green corrosion inhibitor of mild steel in hydrochloric acid medium. *Corros. Commun.* **2024**, *15*, 52–62.

[17]. Mohammed, H. K.; Jafar, S. A.; Humadi, J. I.; Sehgal, S.; Saxena, K. K.; Abdullah, G. H.; Saeed, L. I.; Salman, M. S.; Abdullah, W. S. Investigation of carbon steel corrosion rate in different acidic environments. *Materials Today: Proceedings* **2023**, https://doi.org/10.1016/j.matpr.2023.03.792.

[18]. Alamiery, A. A.; Wan Isahak, W. N.; Takriff, M. S. Inhibition of Mild Steel Corrosion by 4-benzyl-1-(4-oxo-4-phenylbutanoyl)thiosemicarbazide: Gravimetrical, Adsorption and Theoretical Studies. *Lubricants* **2021**, *9* (9), 93.

[19]. Sykes, J. M. Silver Jubilee review 25 years of progress in electrochemical methods. *British Corros. J.* **1990**, *25* (3), 175–183.

[20]. Konovalova, V. The effect of temperature on the corrosion rate of iron-carbon alloys. *Materials Today: Proceedings* **2021**, *38*, 1326–1329.

[21]. Laurent, C.; Scenini, F.; Monetta, T.; Bellucci, F.; Curioni, M. The contribution of hydrogen evolution processes during corrosion of aluminium and aluminium alloys investigated by potentiodynamic polarisation coupled with real-time hydrogen measurement. *NPJ. Mater. Degrad.* **2017**, *1* (1), https://doi.org/10.1038/s41529-017-0011-4.

[22]. Gürten, A. A.; Keleş, H.; Bayol, E.; Kandemirli, F. The effect of temperature and concentration on the inhibition of acid corrosion of carbon steel by newly synthesized Schiff base. *J. Ind. Eng. Chem.* **2015**, *27*, 68–78.

[23]. Noor, E. A. Temperature effects on the corrosion inhibition of mild steel in acidic solutions by aqueous extract of fenugreek leaves. *Int. J. Electrochem. Sci.* **2007**, *2*, 996–1017.

[24]. Şahin, M.; Bilgiç, S.; Yılmaz, H. The inhibition effects of some cyclic nitrogen compounds on the corrosion of the steel in NaCl mediums. *Appl. Surf. Sci.* **2002**, *195*, 1–7.

[25]. Kokalj, A. On the use of the Langmuir and other adsorption isotherms in corrosion inhibition. *Corros. Sci.* **2023**, *217*, 111112.

[26]. Temkin, M. I. The kinetics of some industrial heterogeneous catalytic reactions. In Advances in Catalysis; Elsevier, 1979; pp. 173–291.

[27]. Frumkin, A. Die Kapillarkurve der höheren Fettsäuren und die Zustandsgleichung der Oberflächenschicht. *Z. Phys. Chem.* **1925**, *116U* (1), 466–484.

[28]. Bockris, J. O.; Reddy, A. K. N.; Gamboa-Adelco, M. E. Modern Electrochemistry 2A: Fundamentals of Electrodics; 2nd ed.; Kluwer Academic/Plenum: New York, NY, 2001.

[29]. Olivares, O.; Likhanova, N.; Gómez, B.; Navarrete, J.; Llanos-Serrano, M.; Arce, E.; Hallen, J. Electrochemical and XPS studies of decylamides of α-amino acids adsorption on carbon steel in acidic environment. *Appl. Surf. Sci.* **2006**, *252* (8), 2894–2909.

[30]. Adamu, A. A.; Iyun, O. R.; Habila, J. D. Adsorption and thermodynamic studies of the corrosion Inhibition effect of Desmodium adscendens (Swartz) extract on carbon steel in 2 M HCl. *BMC Chem.* **2025**, *19* (1), https://doi.org/10.1186/s13065-025-01541-y.

[31]. Lin, B.; Shao, J.; Xu, Y.; Lai, Y.; Zhao, Z. Adsorption and corrosion of renewable inhibitor of Pomelo peel extract for mild steel in phosphoric acid solution. *Arab. J. Chem.* **2021**, *14* (5), 103114.

[32]. Hosseini, M.; Mertens, S. F. L.; Arshadi, M. R. Synergism and antagonism in mild steel corrosion inhibition by sodium dodecylbenzenesulphonate and hexamethylenetetramine. *Corros. Sci.* **2003**, *45*, 1473–1489.

[33]. Fateh, A.; Aliofkhazraei, M.; Rezvanian, A. Review of corrosive environments for copper and its corrosion inhibitors. *Arab. J. Chem.* **2020**, *13* (1), 481–544.

[34]. Li, W.; He, Q.; Zhang, S.; Pei, C.; Hou, B. Some new triazole derivatives as inhibitors for mild steel corrosion in acidic medium. *J. Appl. Electrochem.* **2007**, *38* (3), 289–295.

[35]. Bardal, E. Corrosion and Protection; Bardal, E., Ed.; 2004th ed.; Springer: London, England, 2004.

[36]. Atkins, P.; Overton, T.; Rourke, J.; Weller, M.; Armstrong, F. Shriver and Atkins' inorganic chemistry; 5th ed.; Oxford University Press: London, England, 2009.

[37]. Elgyar, O. A.; Ouf, A.; El-Hossiany, A.; Fouda, A. The inhibition action of Viscum album extract on theCorrosion of carbon steel in hydrochloric acid solution. *Biointerface Res. Appl. Chem.* **2021**, *11*, 14344–14358.

[38]. Borowiak-Resterna, A.; Klonowska, K.; Olszanowski, A.; Tomaszewska, M. Photostability of hydrophobic amides of pyridinecarboxylic acid as copper extractants from chloride media. *J. Photochem. Photobiol. A: Chem.* **2007**, *185* (2-3), 181–187.

[39]. Rauța, D. I.; Matei, E.; Avramescu, S. Recent Development of Corrosion Inhibitors: Types, Mechanisms, Electrochemical Behavior, Efficiency, and Environmental Impact. *Technologies* **2025**, *13* (3), 103.

[40]. Liu, J.; Wang, B.; Chen, T.; Hao, L.; Wu, J.; Liu, C. The Effect of Corrosion Inhibitors on the Corrosion Behavior of Ductile Cast Iron. *Metals* **2025**, *15* (1), 70.

[41]. Lee, K.; Sun, S.; Lee, G.; Yoon, G.; Kim, D.; Hwang, J.; Jeong, H.; Song, T.; Paik, U. Galvanic corrosion inhibition from aspect of bonding orbital

theory in Cu/Ru barrier CMP. *Sci. Rep.* **2021**, *11* (1), https://doi.org/10.1038/s41598-021-00689-6.

[42]. Boutouil, A.; Laamari, M. R.; Elazhary, I.; Bahsis, L.; Anane, H.; Stiriba, S. Towards a deeper understanding of the inhibition mechanism of a new 1,2,3-triazole derivative for mild steel corrosion in the hydrochloric acid solution using coupled experimental and theoretical methods. *Mater. Chem. Phys.* **2020**, *241*, 122420.

[43]. Galleguillos Madrid, F. M.; Soliz, A.; Cáceres, L.; Bergendahl, M.; Leiva-Guajardo, S.; Portillo, C.; Olivares, D.; Toro, N.; Jimenez-Arevalo, V.; Páez, M. Green corrosion inhibitors for metal and alloys protection in contact with aqueous saline. Materials (Basel) 2024, 17, 3996.

[44]. Kumar, S. L. A.; Iniyavan, P.; Kumar, M. S.; Sreekanth, A. Corrosion Inhibition Studies of Ecbolium Viride Extracts on Mild Steel in HCl. *J. Mater. Environ. Sci*. **2012**, *3* (3), 461–468.

[45]. Stern, M.; Geaby, A. L. Electrochemical Polarization. *J. Electrochem. Soc.* **1957**, *104* (1), 56.

[46]. Kumar, S. L.; Gopiraman, M.; Kumar, M. S.; Sreekanth, A. 2-Acetylpyridine-*N*(4)-Morpholine Thiosemicarbazone (HAcpMTSc) as a Corrosion Inhibitor on Mild Steel in HCl. *Ind. Eng. Chem. Res.* **2011**, *50* (13), 7824–7832.

[47]. Abdallah, M. Rhodanine azosulpha drugs as corrosion inhibitors for corrosion of 304 stainless steel in hydrochloric acid solution. *Corros. Sci.* **2002**, *44*, 717–728.

[48]. Hermas, A.; Morad, M.; Wahdan, M. Effect of PgTPhPBr on the electrochemical and corrosion behaviour of 304 stainless steel in H2SO4 solution. *J. Appl. Electrochem.* **2004**, *34* (1), 95–102.

[49]. Popova, A.; Raicheva, S.; Sokolova, E.; Christov, M. Frequency Dispersion of the Interfacial Impedance at Mild Steel Corrosion in Acid Media in the Presence of Benzimidazole Derivatives. *Langmuir* **1996**, *12* (8), 2083–2089.

[50]. Larabi, L.; Harek, Y.; Traisnel, M.; Mansri, A. Synergistic Influence of Poly(4-Vinylpyridine) and Potassium Iodide on Inhibition of Corrosion of Mild Steel in 1M HCl. *J. Appl. Electrochem.* **2004**, *34* (8), 833–839.